*Letter to the Editor*

# Extragalactic 2–10 keV source counts from a fluctuation analysis of deep BeppoSAX MECS images

**M. Perri**[1,2] **and P. Giommi**[1]

[1] *Beppo*SAX Science Data Center, ASI, Via Corcolle, 19, 00131 Roma, Italy
[2] Università di Roma "Tor Vergata", Dipartimento di Fisica, Via della Ricerca Scientifica, 1, 00133 Roma, Italy

**Abstract.** We present an analysis of the spatial fluctuations of the 2-10 keV Cosmic X-ray Background (CXB) as measured from 22 high galactic latitude ($|b| > 25°$) fields observed with the MECS instrument on-board *Beppo*SAX. This technique allowed us to probe extragalactic source counts a factor 3-4 fainter than is possible with direct measurements of point-like sources in MECS deep fields. The slope of the 2-10 keV $\log N$-$\log S$ relationship is found to be still close to the "Euclidean" one ($\gamma = 1.5$) down to our flux limit of $\sim 1.5 \times 10^{-14}$ $erg\ cm^{-2}\ s^{-1}$ , where the contribution of discrete sources to the 2-10 keV CXB amounts to $\sim 40 - 50\%$. Source counts derived from the analysis presented in this letter are in very good agreement both with those directly measured with *ASCA* and *Beppo*SAX deep surveys at bright fluxes and with a first estimation of the 2-10 keV *Chandra* $\log N$-$\log S$ at fainter fluxes.

**Key words:** methods: statistical – galaxies: active – cosmology: diffuse radiation – X-rays: general

## 1. Introduction

The understanding of the origin of the Cosmic X-ray Background (CXB, Giacconi et al. 1962) has been and still is one of the main topics of X-ray astronomy. It is now widely accepted that the CXB is the results of the superposition of the emission of faint extragalactic discrete sources and many surveys of the X-ray sky have been carried out to directly resolve the CXB and study the nature of these sources.

The soft X-ray energy band (0.5-2 keV) has been extensively investigated with *ROSAT* with which a large fraction of the soft CXB ($70 - 80\%$) has been resolved into discrete sources (Hasinger et al. 1993, 1998). Spectroscopic identifications of their optical counterparts have revealed that the large majority ($> 80\%$) are AGNs, mostly with broad emission lines (Schmidt et al. 1998).

The harder 2-10 keV sky has become accessible to deep surveys only over the past few years thanks to the imaging in-

struments of *ASCA* and *Beppo*SAX. About 30% of the CXB in this band has been directly resolved into discrete sources and the $\log N$-$\log S$ relationship has been derived down to a flux limit of $\sim 5 \times 10^{-14}$ $erg\ cm^{-2}\ s^{-1}$ (Ueda et al. 1998; Cagnoni, Della Ceca & Maccacaro 1998; Giommi et al. 1998; Della Ceca et al. 1999; Ueda et al. 1999a, 1999b; Fiore et al. 1999; Giommi, Fiore & Perri 1999; Fiore et al. 2000a; Giommi, Perri & Fiore 2000).
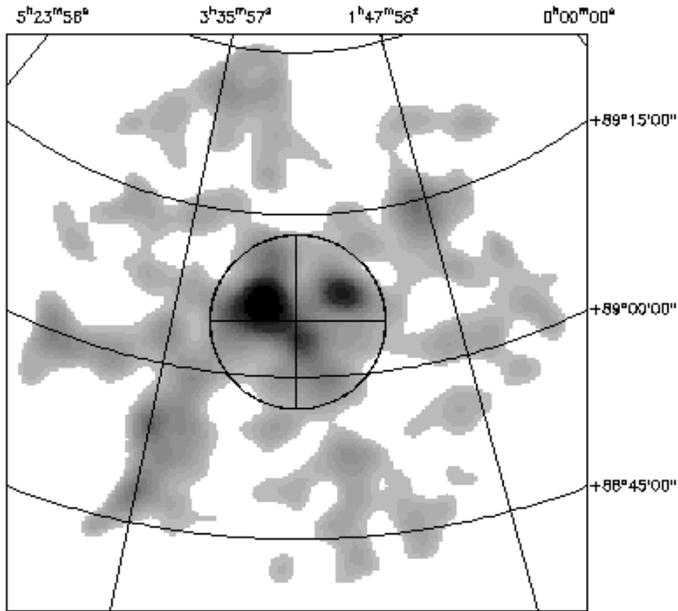
A number of deeper surveys carried out with *Chandra* are now starting to probe the 2-10 keV CXB at much fainter fluxes. However, at least for some time, these can only cover a small area of sky with the consequence that the statistics on source counts (and optical identifications) is still very limited (Brandt et al. 2000; Fiore et al. 2000b; Mushotzky et al. 2000; Hornschemeier et al. 2000).

In this letter we present the results of a fluctuation analysis of *Beppo*SAX MECS images performed in the 2-10 keV energy band that allowed us to study the $\log N$-$\log S$ down to fluxes of $\sim 1.5 \times 10^{-14}$ $erg\ cm^{-2}\ s^{-1}$ . The analysis of the spatial fluctuations of the CXB is a powerful method that allows us to investigate the $\log N$-$\log S$ relationship beyond the flux limit where single sources became too faint, or confused, to be directly detected. The theory behind this technique has been described for the first time by radio astronomers (Scheuer 1957, 1974; Condon 1974) and many applications of this method to X-ray data have successfully predicted source counts at faint fluxes (Hamilton & Helfand 1987; Barcons & Fabian 1990; Hasinger et al. 1993; Barcons et al. 1994; Butcher et al. 1997; Gendreau, Barcons & Fabian 1998). Basically, the method consists of i) comparing the observed spatial fluctuations distribution of the CXB with a set of model distribution curves corresponding to different hypotheses on the power law slope $\gamma$ and normalization $K$ of the $\log N$-$\log S$ relationship and ii) by means of a fitting procedure deriving best fit parameters on source counts.

The main contribution to the observed CXB spatial fluctuations comes from sources at a flux level $S$ corresponding to a source density of about 1-2 sources per beam (Scheuer 1974). This condition determines the sensitivity limit of this technique.

---

*Send offprint requests to*: M. Perri

**Fig. 1.** MECS 2-10 keV image of one of the "blank" fields used in our analysis. The 4 equal quadrants in which the central 8 arcminutes circular region has been divided are also shown.

## 2. Data analysis

The instruments aboard the *Beppo*SAX Satellite (Boella et al. 1997a) include a Low Energy (0.1-10 keV) Concentrator Spectrometer (LECS, Parmar et al. 1997), a Medium Energy (1.3-10 keV) Concentrator Spectrometer composed by three units (MECS, Boella et al. 1997b), a High Pressure Gas Scintillation Proportional Counter (3-120 keV) (HPGSPC, Manzo et al. 1997) and the Phoswich Detector System (15-300 keV) (PDS, Frontera et al. 1997). All these instruments point in the same direction and are collectively called Narrow Field Instruments (NFIs). In addition *Beppo*SAX carries two wide field ($20 \times 20$ degrees FWHM) instruments operating in the 2-30 keV energy band (Wide Field Cameras, WFC, Jager et al. 1997) and pointing in diametrically opposed directions perpendicular to the NFIs.

The data used in our fluctuation analysis consist of 22 non-overlapping high galactic latitude ($|b| > 25°$) MECS fields pointed at "blank" parts of the sky, that is not centered on previously known X-ray targets. About half (13) of these fields are Secondary Pointing NFIs observations, produced when the primary target (usually the Galactic Center) was observed with one of the Wide Field Cameras. The other observations include 3 non-overlapping fields centered near Polaris, the *Beppo*SAX default pointing position in case of safe mode, 2 follow-up observations of Gamma Ray Bursts (GRBs) carried out early in the mission in which X-ray afterglows of the GRBs were not detected, 3 images, taken from the public archive, not centered on known X-ray sources, and 1 image taken during the Leonids meteorites crossing on November 17, 1999, when the satellite was oriented so as to minimize the probability of impact with one of the meteorites. The average exposure of the 22 fields

is $\sim 88$ ks while typical values of galactic $N_H$, as derived by the 21 cm measurements of Dickey & Lockman (1990), are $\sim 4 \times 10^{20}$ cm$^{-2}$. No point sources with 2-10 keV flux greater than $5 \times 10^{-13}$ erg cm$^{-2}$ s$^{-1}$ are detected in any of these fields.

As discussed above, the MECS instruments is composed of three nearly identical units. One of these (MECS1) failed on May 7th 1997. To ensure uniformity we have used data only from the units MECS2 and MECS3, to which we refer hereafter as the MECS instrument. To avoid difficulties due to complex variations in sensitivity across the field-of-view (FOV) we have restricted our analysis to the central 8 arcminutes circular regions (see Fig. 1) where the sensitivity is higher and vignetting and Point Spread Function (PSF) variations are small.
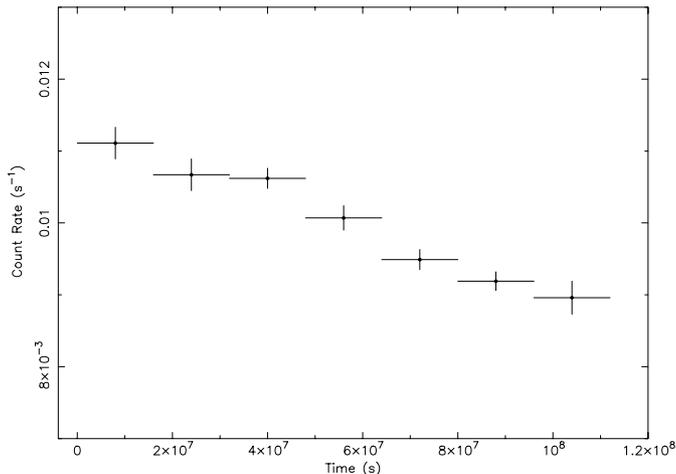
In order to enhance the sensitivity of our analysis as well the statistics of the CXB granularity each circular region has been divided in 4 equal quadrants (each covering an area of $\sim 50.3$ arcmin$^2$, see Fig. 1) for a total of 88 independent measurements of the CXB. This sets our sensitivity to $S \sim 1.5 \times 10^{-14}$ erg cm$^{-2}$ s$^{-1}$ , the exact value depending on the details of the log$N$-log$S$ relationship. At this flux level one source corresponds to $\sim 10 - 15$ MECS net counts, well above the "1 photon per source limit" which is considered as a further limit of the fluctuation analysis method.

### 2.1. The non X-ray background

To estimate the amount of cosmic X-rays we must subtract the non X-ray background (NXB, that is the instrument noise plus the particle background) which, in the central 8 arcminutes of the MECS, accounts for about half of the total counts.

To measure the NXB we have used, as in Parmar et al. (1999) and in Vecchi et al. (1999), *Beppo*SAX MECS "dark Earth fields", that is MECS images taken when the pointing direction is occulted by the part of the Earth that is not illuminated by the Sun. We have accumulated "dark Earth" observations from July 1996 through September 1999 for a total exposure time of 3.85 Ms. Counts between channels 44 and 200 (the energy range used to estimate the CXB, see below) have been extracted from the inner 8 arcminutes circular regions of the images. The corresponding MECS light curve is shown in Fig. 2. A gradual decline of the count rate with time is evident. From July 1996 to September 1999 the amount of this reduction is $\sim 15 - 20\%$. We modeled this behaviour with the law $cr(t) = cr(0) - 2.07 \times 10^{-11} \times t$, where $t$ is time in seconds and $cr(0) \simeq 1.11 \times 10^{-2}$ s$^{-1}$ is the NXB count rate value at the beginning of the mission ($t = 0$, 1996 July 6). A similar instrumental background reduction has been reported for the LECS instrument on-board *Beppo*SAX by Parmar et al. (1999).

We also investigated potential systematic errors in the estimation of the NXB, such as significant deviations of count rate from the law given above or the statistical poisson noise of the NXB counts in a MECS quadrant. In both cases, given the typical exposure times of our MECS fields ($T \simeq 90$ ks), such effects are negligible with respects to the measured fluctuations of the net counts.

**Fig. 2.** MECS Non X-ray Background count rate (channels 44-200, central 8 arcminutes circular regions) as a function of time. "Dark Earth" data have been accumulated from 1996 July 6 ($t = 0$) to 1999 September 11 for a total exposure time of 3.85 Ms.



**Fig. 3.** Distribution of the 2-10 keV Cosmic X-ray Background measurements (histogram). The best fit model curve from our ML estimation (solid line) is also shown.
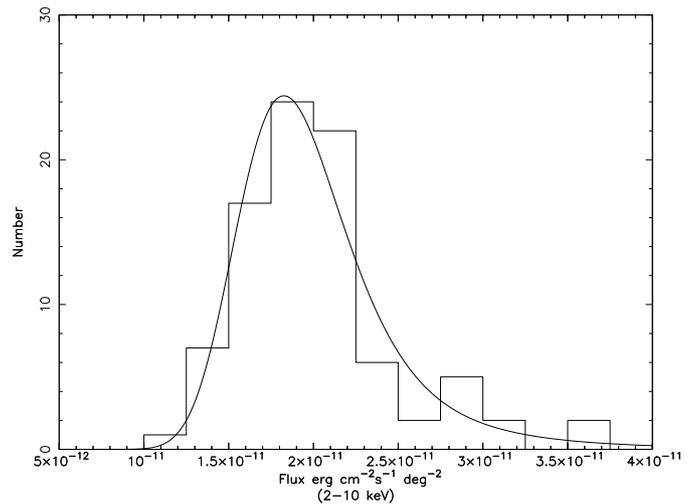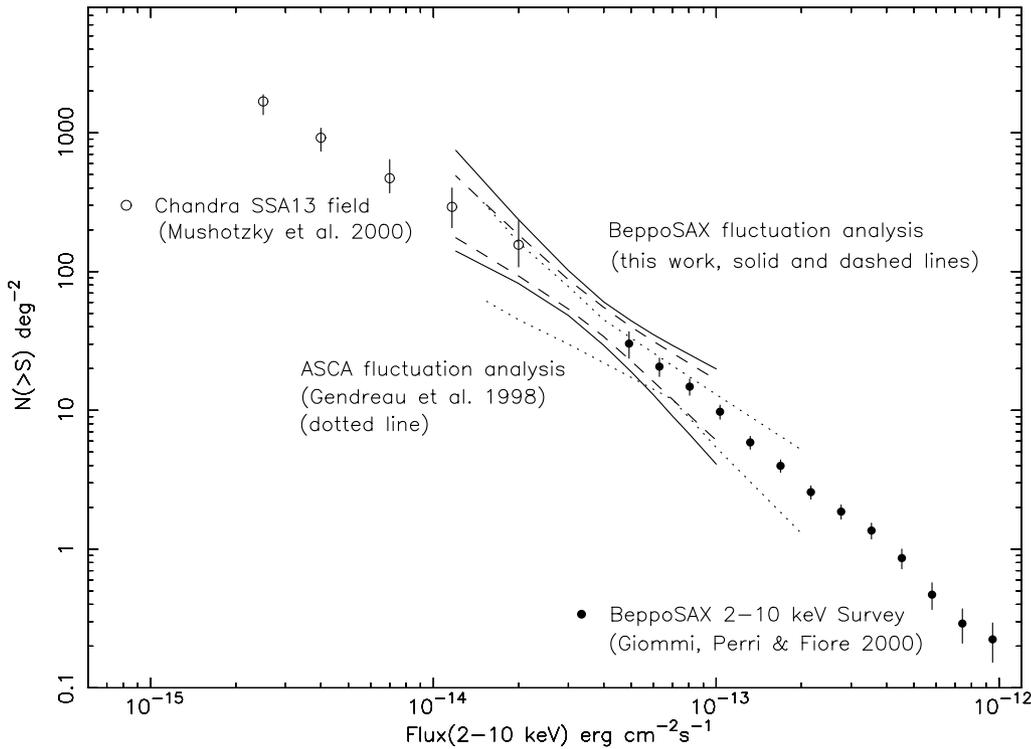
### 2.2. The CXB flux distribution

Net counts between channels 44 and 200 (2.0-9.0 keV) have been extracted from the central 8 arcminutes quadrants of the 22 "blank" fields and converted to fluxes in the 2-10 keV band. A power law spectrum with energy index $\alpha \simeq 0.6$ has been assumed, as indicated by *ASCA* and *Beppo*SAX deep 2-10 keV X-ray surveys (Ueda et al. 1999b; Giommi, Perri & Fiore 2000). Corrections for the Galactic absorbing neutral hydrogen column density $N_H$ have also been applied. Counts in the channel range 200-220 (9.0-10.0 keV) have been excluded since the NXB dominates this energy band. The flux distribution of the 88 independent measurements of the Cosmic X-ray Background is shown in Fig. 3. The average flux is $\simeq 2.3 \times 10^{-11}$ $erg\ cm^{-2}\ s^{-1}\ deg^{-2}$, a value that is $\sim 35\%$ higher than that of HEAO1 (Marshall et al. 1980) and slightly higher ($\sim 15\%$) than the *ASCA* GIS value (Miyaji et al. 1998) but in good agreement with the Wisconsin rocket data (McCammon & Sanders 1990 and references therein) and with the MECS measurement obtained from a smaller data sample by Vecchi et al. (1999).

### 3. Fluctuation analysis

To compute the predicted CXB spatial fluctuations we have adopted an analytical approach that, besides the statistical fluctuations due to the expected number of X-ray sources, includes counting statistics and the effects of MECS vignetting and PSF.

Our method can be summarized as follows. A power law form for the $\log N$-$\log S$ relationship is assumed, $N(> S) = K\ (S/S_0)^{-\gamma}$, where $K$ is the number of sources per unit area with flux $S > S_0$.

The expected number $\bar{N}$ of sources in one beam (one MECS quadrant) in the flux range from $\bar{S}$ to $\bar{S} + dS$ is then obtained simply multiplying the differential of the $\log N$-$\log S$ with the area of a MECS quadrant. Next, the probability of a fluctuation of the number of sources is computed assuming Poisson statis-

tics and the corresponding photon counts distribution. Counting statistics and vignetting effects are included in the procedure by means of two independent probability convolutions with i) the Poisson distribution of counts themselves and ii) the off-axis angles probability distribution of sources in the MECS FOV. Probability convolutions have been computed by means of a Fast Fourier Transform (FFT) technique.

The 2-10 keV MECS PSF size (the radius where 80% of the photons are collected is $\sim$ 2.6 arcminutes, Boella et al. 1997b) is non-negligible compared to the regions were we extract counts and consequently photons due to sources just outside the 8 arcminutes quadrant cannot be neglected. Similarly to the *ASCA* fluctuation analysis of Gendreau, Barcons & Fabian (1998) we have then divided a MECS quadrant and "nearby regions" with 2 arcminutes size boxes and computed the fraction of photons that fall inside a quadrant at different FOV positions. We have next constructed the off-axis angles probability distribution of sources and included this effect with a further convolution. This procedure is repeated for all fluxes between $S_{\min}$, the flux at which the $\log N$-$\log S$ integrated intensity exceeds the CXB value (as estimated in Vecchi et al. 1999), and $S_{\max} = 5 \times 10^{-13}\ erg\ cm^{-2}\ s^{-1}$ (sources with $S > S_{\max}$ are absent from our data and do not contribute to the CXB fluctuations). Finally, from the probability convolution of the computed flux distributions we obtain the expected distribution of CXB spatial fluctuations corresponding to the assumed values of $\gamma$ and $K$.

We have compared the observed CXB spatial fluctuations with a set of model curves computed assuming different trial $\log N$-$\log S$ relationships. A maximum likelihood (ML) test has been used to estimate the best fit, 68% and 90%, ($\Delta S = 2.3$ and 4.6) constraints on the 2-10 keV $\log N$-$\log S$ power law slope $\gamma$ and normalization $K$ (as defined by Eq. (2) with $S_0 = 1 \times 10^{-14}$ $erg\ cm^{-2}\ s^{-1}$ ). The best fit values are $\gamma = 1.5 \pm 0.2$ and $K = 336^{+114}_{-58}\ deg^{-2}$ where the quoted errors correspond to 90% confidence level for one interesting parameter ($\Delta S = 2.7$).

**Fig. 4.** 2-10 keV integral source counts. Solid and dashed "bow tie" regions are 90% and 68% contours from the present *Beppo*SAX fluctuation analysis. Dotted lines are the 1 $\sigma$ contours from the *ASCA* fluctuation analysis of Gendreau, Barcons & Fabian (1998). Filled circles represent the *Beppo*SAX 2-10 keV $\log N$-$\log S$ relationship (Giommi, Perri & Fiore 2000) and open circles are *Chandra* source counts from the SSA13 field (Mushotzky et al. 2000).

The solid line in Fig. 3 shows the model best-fit flux distribution which approximates well the observed one (a Kolmogorov-Smirnov test gives a probability $> 95\%$ that the two distributions are equal).

The 90% and 68% constraints of our fluctuation analysis on the 2-10 keV integral $\log N$-$\log S$ are shown in Fig. 4. For comparison the 1 $\sigma$ contours from the *ASCA* SIS fluctuation analysis of Gendreau, Barcons & Fabian (1998) and 2-10 keV source counts from *Beppo*SAX (Giommi, Perri & Fiore 2000) and *Chandra* (Mushotzky et al. 2000) surveys are also plotted.

## 4. Simulations

In order to check our procedure we have carried out extensive simulations of MECS images using the data simulator available at the *Beppo*SAX Science Data Center (Giommi & Fiore 1997). This tool fully includes MECS instrumental features as telescope vignetting, PSF shape, non X-ray background and Poisson noise.

We generated 3 sets of one hundred MECS images with pointlike sources following 3 different $\log N$-$\log S$ distributions. Sources have been simulated in the flux range $S_{\min} - S_{\max}$ (see above) with exposure time $T = 90$ k$s$.

Each set of simulated images have been analyzed following the same procedure used for the real data. The resulting flux distributions have then been compared with the model curves and the maximum likelihood test performed.

We have found that the input values for the power law slope $\gamma$ and the normalization $K$ of the $\log N$-$\log S$ are in all 3 cases within the 68% confidence contours of the fitted ones indicating that no significant bias in their estimation affects our analysis.

## 5. Summary and conclusions

We have performed a CXB fluctuation analysis based on 22 non-overlapping high galactic latitude ($|b| > 25°$) MECS images of "blank" parts of the sky. The total exposure time is $\simeq 1.94$ M$s$ while the area covered is $\simeq 1.23 \deg^2$. The analysis of the CXB spatial fluctuations has allowed us to extend the 2-10 keV $\log N$-$\log S$ relationship down to fluxes $\sim 1.5 \times 10^{-14} \, erg \, cm^{-2} \, s^{-1}$. At this flux level the contribution of discrete sources to the 2-10 keV Cosmic X-ray Background is $\sim 40 - 50\%$. The best fit values for the slope $\gamma$ and the normalization $K$ of the $\log N$-$\log S$ are $\gamma = 1.5 \pm 0.2$ and $K = 336^{+114}_{-58} \deg^{-2}$ (quoted errors correspond to 90% confidence level). Fig. 4 summarizes our results. A good agreement with the *ASCA* fluctuation analysis of Gendreau, Barcons & Fabian (1998) and with *Beppo*SAX direct source counts at bright fluxes (Giommi, Perri & Fiore 2000) and a first estimate of the *Chandra* 2-10 keV $\log N$-$\log S$ (Mushotzky et al. 2000) at faint fluxes is found.

## References

Barcons X., Fabian A.C., 1990, MNRAS 243, 366

Barcons X., Branduardi-Raymont G., Warwick R.S. et al., 1994, MN-RAS 268, 833

Boella G., Butler R.C., Perola G.C. et al., 1997a, A&AS 122, 299

Boella G., Chiappetti L., Conti G. et al., 1997b, A&AS 122, 327

Brandt W.N., Hornschemeier A.E., Schneider D.P. et al., 2000, AJ, in press (astro-ph/0002121)

Butcher J.A., Stewart G.C., Warwick R.S. et al., 1997, MNRAS 291, 437

Cagnoni I., Della Ceca R., Maccacaro T., 1998, ApJ 493, 54

Condon J.J., 1974, ApJ 188, 279

Della Ceca R., Castelli G., Braito V. et al., 1999, ApJ 524, 674

Dickey J.M., Lockman F.J., 1990, ARA&A 28, 215

Fiore F., La Franca F., Giommi P. et al., 1999, MNRAS 306, L55

Fiore F., Giommi P., Vignali C. et al., 2000a, MNRAS, submitted

Fiore F., La Franca F., Vignali C. et al., 2000b, New Astronomy, in press (astro-ph/0003273)

Frontera F., Costa E., Dal Fiume D. et al., 1997, A&AS 122, 371

Gendreau K.C., Barcons X., Fabian A.C., 1998, MNRAS 297, 41

Giacconi R., Gursky H., Paolini F., Rossi B., 1962, Phys. Rev. Lett. 9, 439

Giommi P., Fiore F., 1997, Proc. of "5th International Workshop on Data Analysis in Astronomy", Erice, Italy

Giommi P., Fiore F., Ricci D. et al., 1998, Nucl. Phys. B 69/1-3, 591

Giommi P., Fiore F., Perri M., 1999, Astrophys. Letters & Communications, Vol. 39, 173 (astro-ph/9812305)

Giommi P., Perri M., Fiore F., 2000, A&A, in press

Hamilton T.T., Helfand D.J., 1987, ApJ 318, 93

Hasinger G., Burg R., Giacconi R. et al., 1993, A&A 275, 1

Hasinger G., Burg R., Giacconi R. et al., 1998, A&A 329, 482

Hornschemeier A.E., Brandt W.N., Garmire G.P. et al., 2000, ApJ in press (astro-ph/0004260)

Jager R., Mels W.A., Brinkman A.C. et al., 1997, A&AS 125, 557

Manzo G., Giarusso S., Santangelo A. et al., 1997, A&AS 122, 341

Marshall F.E., Boldt E.A., Holt S.S. et al., 1980, ApJ 235, 4

McCammon D., Sanders W.T., 1990, ARA&A 28, 657

Miyaji T., Ishisaki Y., Ogasaka Y. et al., 1998, A&A 334, L13

Mushotzky R.F., Cowie L.L., Barger A.J., Arnaud K.A., 2000, Nature 404, 459

Parmar A.N., Martin D.D.E., Bavdaz M. et al., 1997, A&AS 122, 309

Parmar A.N., Oosterbroek T., Orr A. et al., 1999, A&AS 136, 407

Scheuer P.A.G., 1957, Proc. Cambridge Phil. Soc. 53, 764

Scheuer P.A.G., 1974, MNRAS 166, 329

Schmidt M., Hasinger G., Gunn J. et al., 1998, A&A 329, 495

Ueda Y., Takahashi Y., Inoue H. et al., 1998, Nature 391, 866

Ueda Y., Takahashi Y., Inoue H. et al., 1999a, ApJ 518, 656

Ueda Y., Takahashi Y., Ishisaki Y. et al., 1999b, ApJ 524, L11

Vecchi A., Molendi S., Guainazzi M. et al., 1999, A&A 349, L73